Temperature insensitive fluorescence intensity in a coumarin monomer–aggregate coupled system†

Xiaogang Liu,‡[a] Deqi Mao,‡[bc] Jacqueline M. Cole*[ad] and Zhaochao Xu*[bc]

The emission intensities of a fluorescent monomer–aggregate coupled system, based on 7-(dimethylamino)-coumarin-3-carbaldehyde, exhibit ultra-low temperature dependence with a low temperature coefficient of only 0.05% per °C, by judicious selection of the excitation wavelength. This finding has significant implications to temperature-sensitive fluorescent applications.

Fluorescent probes are essential tools in many applications, such as tracking cellular events in biological systems,[1] investigating the distribution and activity of catalytic zeolite particulates[2] and exploring the flow mixing in fluid dynamics.[3] Their high spatial resolution and quick response characteristics also make them particularly attractive in the study of micro-systems.[4] However, the effect of temperature variation on the photophysics and photochemistry of fluorescent probes has often been ignored, despite being a crucial factor for an accurate interpretation of fluorescent signals.[5] Fluorescence intensities or quantum efficiencies (QE) decrease with a rise in temperature in almost all fluorescent systems, owing to the increasing frequency of dye-solvent collisions and the internal rotations/vibrations of dye molecules; this results in higher nonradiative de-excitation rates. Recent studies have shown that the distribution of temperature is highly heterogeneous and dynamic in cells[6,7] and microfluidic devices.[8] Therefore, during the quantitative analysis of fluorescent signals, the cross-sensitivity of a probe to temperature (in addition to target species/processes) must be considered or, preferably, avoided through the use of a temperature-independent fluorescent system.

This system can also serve as a reference dye (or built-in correction) for temperature sensing and temperature effect correction in conjunction with other temperature sensitive dyes.[4] To date, wholly temperature insensitive dyes are unattainable; the lowest temperature-dependence in a fluorescence system requests the use of certain rigid dyes, such as rhodamine 101. However, this dye possesses a temperature coefficient of 0.13% per °C at 20 °C, or ∼6% intensity variation over a temperature change of 50 °C.[9] Developing a fluorescent system with an ultra-low temperature coefficient remains a challenging task.

Following the recent exploration of molecular aggregates and their functionalities,[10–24] we propose and demonstrate a new design concept to achieve ultra-low temperature dependence of emission intensity using a monomer–aggregate coupled system. In the most simplified version of this design, the QE of a dye drops as temperature increases; while at the same time, the rising temperature leads to the dissolution of non-emissive molecular aggregates, boosting the quantity of emissive monomers. By achieving a proper balance between these two contrasting temperature dependent emission characteristics, the overall emission intensity of the fluorescent system could be maintained at a constant level. However, the actual picture could be more complicated, since different phases of aggregates may co-exist and some molecular aggregates are highly emissive, whilst most of them are non- or weakly fluorescent.

Our model system is based on 7-(dimethylamino)-coumarin-3-carbaldehyde (**1**) in chloroform (Scheme S1; Fig. S1–S5, ESI†). Cigáň *et al.* showed that this dye formed highly emissive H-aggregates in methanol and ethanol, but they did not observe molecular aggregates in several other solvents, such as CHCl$_3$ and ethyl acetate (EA).[25] However, we find that emissive H-aggregates exist in CHCl$_3$, EA, and several other solvents tested in-house, including cyclohexane, toluene, tetrahydrofuran (THF), and dimethyl sulfoxide (DMSO). The molecular aggregation in CHCl$_3$ is very subtle, as reflected by the almost perfect match in the normalized UV-Vis absorption spectra of **1** at different concentrations (Fig. 1a). In addition, in the 2D excitation-emission

[a] *Cavendish Laboratory, Department of Physics, University of Cambridge, J. J. Thomson Avenue, Cambridge CB3 0HE, UK. E-mail: jmc61@cam.ac.uk*
[b] *Key Laboratory of Separation Science for Analytical Chemistry, Dalian Institute of Chemical Physics, Chinese Academy of Sciences, 457 Zhongshan Road, Dalian 116023, China. E-mail: zcxu@dicp.ac.cn; Fax: +86-411-84379648*
[c] *State Key Laboratory of Fine Chemicals, Dalian University of Technology, 2 Linggong Road, Dalian 116012, China*
[d] *Argonne National Laboratory, 9700 S Cass Avenue, Argonne, IL 60439, USA*
† Electronic supplementary information (ESI) available: Synthesis, characterization, experimental and computational details. See DOI: 10.1039/c4cc04245j
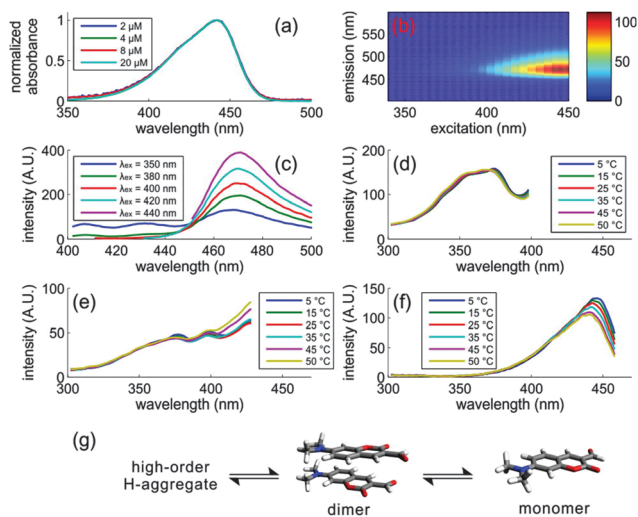‡ These authors contributed equally.

Fig. 1 (a) Normalized UV-Vis absorption spectra of **1** in CHCl₃; (b) 2D excitation–emission map of **1** in CHCl₃ ([**1**] = 2 μM; T = 25 °C); (c) excitation–dependent emission profiles of **1** in CHCl₃ ([**1**] = 2 μM; T = 25 °C); the emission spectra have been scaled arbitrarily for clarity. Fluorescence excitation spectra of **1** in CHCl₃ ([**1**] = 4 μM) at: (d) λ_{em} = 406 nm (slit size = 5 : 10 nm); (e) λ_{em} = 436 nm (slit size = 5 : 5 nm) and (f) λ_{em} = 470 nm (slit size = 2.5 : 2.5 nm). (g) Proposed aggregation model and the calculated structures of the monomer and dimer of **1** in CHCl₃.

Fig. 2 Temperature dependence of fluorescence intensities of **1** ([**1**] = 4 μM; slit size = 2.5 : 2.5 nm) excited at: (a) λ_{ex} = 395 nm; (b) λ_{ex} = 410 nm; (c) λ_{ex} = 415 nm and (d) λ_{ex} = 450 nm in CHCl₃. Temperature dependence (from 5 to 50 °C) of the ratios of fluorescence intensities and the associated best-fit equations (e) at 475 nm, excited at 450 and 410 nm, respectively; (f) at 460 nm, excited at 450 and 410 nm, respectively; (g) at 475 and 460 nm, excited at 410 nm; (h) at 475 and 460 nm, excited at 450 nm. Two vertical lines at 460 and 475 nm are drawn in (b) and (d), respectively, to illustrate the different temperature dependence of the emission intensities at these two wavelengths.

map of **1**, only one significant peak is observed, indicating the presence of just one species in solution (Fig. 1b).

Nevertheless, a closer look, *via* the excitation-dependent emission profiles of **1**, does suggest the presence of molecular aggregates (Fig. 1c). When excited at 350 nm, **1** exhibits two secondary peaks at ∼406 and ∼440 nm, in addition to the main peak at 470 nm. As the excitation shifts to longer wavelengths, the main peak becomes increasingly dominant, rendering the secondary peaks undetectable. The fluorescence excitation spectra were also probed, at the emission wavelengths of 406, 436 and 470 nm. These spectra demonstrate three distinct peaks at ∼370, ∼395 and ∼445 nm, in turn, and suggest the co-existence of three species in the solution of **1** in CHCl₃ (Fig. 1d–f and Fig. S6–S9, ESI†).

These three species are assigned as high-order H-aggregates, low-order H-aggregates (mainly dimers) and monomer units, respectively (Fig. 1g). The absorption band peak at ∼445 nm and the associated emission peak at ∼470 nm exhibit broad profiles, in contrast to the narrow bands indicative of J-aggregates.[26] TD-DFT calculations suggest that these peaks are related to the monomers of **1** (ESI†). The remaining two species in CHCl₃ exhibit blue-shifted peaks, larger Stokes shifts than the monomers of **1** and broad absorption/emission profiles, which are typical characteristics of H-aggregates.[20] Indeed, TD-DFT calculations show that the H-dimer exhibits a hypsochromic shift with respect to the monomer of **1** (ESI†). The presence of H-aggregates in CHCl₃ is not surprising, considering that similar aggregates have been reported in methanol and ethanol.[25] Moreover, slight upfield shifts in the NMR spectra of **1** were also observed as its concentration increased in CHCl₃ and methanol, corroborating our conclusion that molecular aggregates are present (Fig. S10 and S11, ESI†). However, the subtle changes in the molar absorptivity of **1** in CHCl₃ with respect to dye
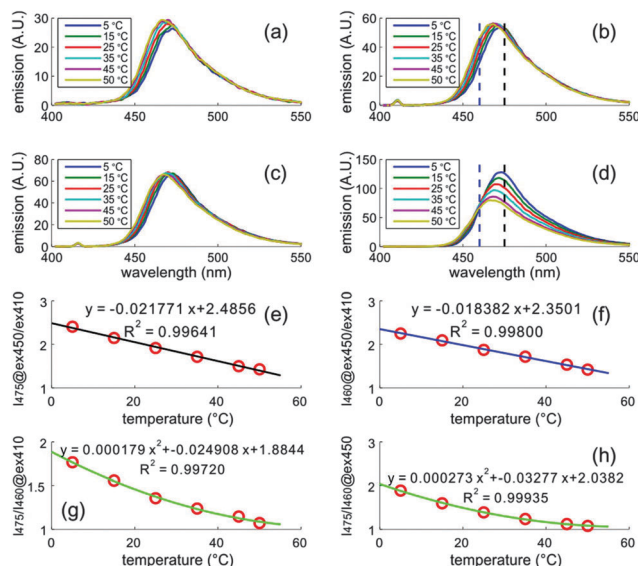
concentration and temperature prevent us from accurately determining the aggregate formation constants.

This coumarin monomer–aggregate coupled system possesses a unique temperature dependence (Fig. 2a–d). While excited at 395 nm, where strong absorption is observed owing to dimer formation, the fluorescence intensity unusually exhibits an increase with rising temperature (Fig. 2a). We attribute this effect to a relatively large increase in dimer quantity (by dissolving high-order aggregates) with respect to the drop in dimer QE. The considerable increase in dimer quantity with temperature is also reflected by a small but consistent blue shift of 3 nm in the UV-Vis absorption spectra of **1** from 5 to 50 °C, towards the dimer absorption peak (Fig. S12–S14, ESI†). In contrast, the under-compensation of monomers leads to a decrease in emission intensity as temperature increases (Fig. 2d). By choosing an intermediate or "optimal" excitation wavelength, *i.e.*, 415 nm, the decrease in monomer emission can be balanced by the intensification of dimer emission. Consequently, the overall emission intensities of this system remain little changed, with a small variation of only ∼3% over a temperature change of 45 °C, or a very low effective temperature coefficient of ∼0.06% per °C (Fig. 2c). As the contribution of dimer emission increases at high temperatures, the peak fluorescent wavelength (λ_f) of **1** also experiences a small blue shift of 5 nm from 5 to 50 °C.

The balance mechanism in the fluorescence intensity of **1** is also revealed *via* fluorescent lifetime measurements. When excited at 405 nm, the fluorescence decay dynamics of emissions between 415 and 475 nm of **1** follows a double-exponential decay with two distinct time-constants of 1.1 and 2.9 ns (Table S1, ESI†).

Table 1 The "optimal" excitation wavelengths and associated fluorescence intensity/peak emission wavelength variations of **1** in CHCl₃ over different concentrations[a]

Concentration (µM)	"Optimal" excitation wavelength (nm)	Intensity variation from 5 to 50 °C (%)	λ_f shift from 5 to 50 °C (nm)
2	415	2.4	5
4	415	3.5	6
8	410	3.5	4
20	410	2.6	4
40	400	2.3	3

[a] The "optimal" excitation wavelength refers to the excitation wavelength affording the minimal fluorescence intensity variations over temperature changes. During the determination of this "optimal" wavelength, the excitation wavelength is varied at a step size of 5 nm across the entire first absorption band of **1**.

They are assigned to dimer and monomer emissions, respectively. According to their varied contributions at different emission wavelengths and the overall emission spectrum, the monomer and dimer emission spectra have been extracted (Fig. S15, ESI†).

Similar effects of temperature insensitive fluorescence intensities are also observed in **1** at higher concentrations (Table 1 and Tables S2 and S3, ESI†). In these samples, the relative weight of monomer emission increases, probably because the low-order aggregates start to grow and their QE decreases accordingly. Therefore, the optimal excitation wavelengths shift towards the dimer absorption peak. However, these shifts are, in general, small, indicating that a fixed excitation wavelength (*i.e.*, 415 nm) can be employed over a wide concentration range to achieve ultra-low temperature dependence in this monomer–aggregate coupled fluorescent system. At 415 nm, the absorptivity of this coumarin monomer–aggregate coupled system amounts to ~1.95×10^4 L mol⁻¹ cm⁻¹ and its QE is ~40%, suggesting good fluorescence brightness.

This temperature dependence was investigated in other solvents. In solvents with similar polarities as compared to CHCl₃, such as EA and THF, it was found that the increase of dimer emission counterbalances the decrease in monomer fluorescence, resulting in very low temperature coefficients at carefully selected excitation wavelengths (0.05 and 0.07% per °C in EA and THF, respectively; Fig. S16 and S17; Tables S4 and S5, ESI†). This suggests that the low temperature dependence is not specific to CHCl₃, but can be realized in other solvents as well. However, in lower polarity solvent (such as cyclohexane and toluene) and higher polarity solvents (such as methanol, ethanol and DMSO), the emission intensities of both monomers and aggregates decrease as temperature increases. Hence, the temperature dependence is relatively high, regardless of the excitation wavelength. These facts are attributed to significant decreases in QE, which cannot be offset by high-order aggregate dissolution.

The ultra-low temperature dependence demonstrated in this monomer–aggregate coupled system of **1** could also be realized with other dyes that are prone to molecular aggregation, and probably in different solvents, *via* controlling the molecular structures of dyes (and their associated steric hindrance effects and electrostatic interactions) and the solvent composition; this essentially determines the thermodynamic parameters

for the monomer–aggregate equilibrium. In fact, we have also found that coumarin 545 possesses similar temperature insensitivity in THF, methanol and DMSO. In particular, its temperature coefficient in methanol is as low as 0.025% per °C. To our best knowledge, this result represents the lowest temperature coefficient among all fluorescence systems reported to date. More details about this compound will be reported in a forthcoming publication.

These systems stand to be useful for temperature-sensitive applications. In particular, they could be employed to monitor solvent temperatures and the associated dynamic processes (such as heat transfer[27,28]) with high spatial and temporal resolution in a contact-less way.[29] In conventional two-color laser-induced fluorescent thermometry, for example, the emission intensity ratio of a temperature-sensitive dye (usually rhodamine B) and a temperature-insensitive reference dye (typically rhodamine 101) is used to derive fluid temperature.[9,30,31] Since these two dyes have different photo-bleaching rates, the reliability of this thermometry can be compromised.[4] In contrast, only one type of dye would be sufficient when employing this monomer–aggregate coupled system. By exciting this system at different wavelengths, distinct temperature dependence at the same emission wavelength, varying from negative to positive temperature coefficients, can be realized, owing to altered contributions from the monomer and dimer emissions (Fig. 2b and d; Tables S1–S5, ESI†); the resulting fluorescent intensity ratios provide valuable information about the solvent temperature (Fig. 2e and f). Similarly, by exciting this monomer–aggregate coupled system at the same wavelength, the ratios of fluorescence intensities at different emission wavelengths can also serve as a temperature indicator (Fig. 2g and h). Interestingly, this temperature sensing functionality is not limited in CHCl₃, but also works in other solvents, such as THF, EA, ethanol and DMSO (Fig. S18–S23, ESI†). The only requirement for such a temperature sensor is the involvement of two emission species with distinct temperature coefficients.

In conclusion, a new design concept to achieve ultra-low temperature dependence in a fluorescent system has been proposed and demonstrated using an equilibrated monomer–aggregate coupled system based on **1**. By balancing the QE variation and the relative quantities of monomers and dimers (which vary due to aggregate formation/dissolution) over different temperatures, the temperature dependence of this system can be adjusted by simply varying excitation wavelengths. While the demonstration of ultra-low temperature dependence has been herein confined to **1** in CHCl₃, EA and THF, it is expected that this design concept can also be extended to other dyes, which probably function in a different set of solvents, such as aqueous solution, thus enabling a new and diverse range of temperature-sensitive fluorescent applications. In addition, it has been demonstrated that the monomer–aggregate coupled system can be used for temperature sensing applications.

Notes and references

1 J. Zhang, R. E. Campbell, A. Y. Ting and R. Y. Tsien, *Nat. Rev. Mol. Cell Biol.*, 2002, **3**, 906–918.
2 I. L. C. Buurmans, J. Ruiz-Martínez, W. V. Knowles, D. van der Beek, J. A. Bergwerff, E. T. C. Vogt and B. M. Weckhuysen, *Nat. Chem.*, 2011, **3**, 862–867.
3 T. J. Johnson, D. Ross and L. E. Locascio, *Anal. Chem.*, 2001, **74**, 45–51.
4 X.-D. Wang, O. S. Wolfbeis and R. J. Meier, *Chem. Soc. Rev.*, 2013, **42**, 7834–7869.
5 A. E. Oliver, G. A. Baker, R. D. Fugate, F. Tablin and J. H. Crowe, *Biophys. J.*, 2000, **78**, 2116–2126.
6 K. Okabe, N. Inada, C. Gota, Y. Harada, T. Funatsu and S. Uchiyama, *Nat. Commun.*, 2012, **3**, 705.
7 Y. Takei, S. Arai, A. Murata, M. Takabayashi, K. Oyama, S. i. Ishiwata, S. Takeoka and M. Suzuki, *ACS Nano*, 2014, **8**, 198–206.
8 C. Gosse, C. Bergaud and P. Löw, in *Thermal Nanosystems and Nanomaterials*, ed. S. Volz, Springer Berlin Heidelberg, 2009, ch. 10, vol. 118, pp. 301–341.
9 J. Sakakibara and R. Adrian, *Exp. Fluids*, 1999, **26**, 7–15.
10 J. Köhler, *Nat. Chem.*, 2012, **4**, 598–600.
11 E. Gaufrès, N. Y. W. Tang, F. Lapointe, J. Cabana, M. A. Nadon, N. Cottenye, F. Raymond, T. Szkopek and R. Martel, *Nat. Photonics*, 2014, **8**, 72–78.
12 D. Ding, K. Li, B. Liu and B. Z. Tang, *Acc. Chem. Res.*, 2013, **46**, 2441–2453.
13 K. C. Hannah and B. A. Armitage, *Acc. Chem. Res.*, 2004, **37**, 845–853.
14 S. Sengupta and F. Würthner, *Acc. Chem. Res.*, 2013, **46**, 2498–2512.
15 X. Li, H. Liu, X. Sun, G. Bi and G. Zhang, *Adv. Opt. Mater.*, 2013, **1**, 549–553.
16 D. Görl, X. Zhang and F. Würthner, *Angew. Chem., Int. Ed.*, 2012, **51**, 6328–6348.
17 F. Würthner, T. E. Kaiser and C. R. Saha-Möller, *Angew. Chem., Int. Ed.*, 2011, **50**, 3376–3410.
18 S. Yagai, T. Seki, T. Karatsu, A. Kitamura and F. Würthner, *Angew. Chem., Int. Ed.*, 2008, **47**, 3367–3371.
19 F. Bergström, I. Mikhalyov, P. Hägglöf, R. Wortmann, T. Ny and L. B. Å. Johansson, *J. Am. Chem. Soc.*, 2002, **124**, 196–204.
20 F. Fennel, S. Wolter, Z. Xie, P. A. Plötz, O. Kühn, F. Würthner and S. Lochbrunner, *J. Am. Chem. Soc.*, 2013, **135**, 18722–18725.
21 Y. J. Huang, W. J. Ouyang, X. Wu, Z. Li, J. S. Fossey, T. D. James and Y. B. Jiang, *J. Am. Chem. Soc.*, 2013, **135**, 1700–1703.
22 T. E. Kaiser, V. Stepanenko and F. Würthner, *J. Am. Chem. Soc.*, 2009, **131**, 6719–6732.
23 Y. Hong, J. W. Y. Lam and B. Z. Tang, *Chem. Soc. Rev.*, 2011, **40**, 5361–5388.
24 W. Z. Yuan, P. Lu, S. Chen, J. W. Y. Lam, Z. Wang, Y. Liu, H. S. Kwok, M. Yuguang and B. Z. Tang, *Adv. Mater.*, 2010, **22**, 2159–2163.
25 M. Cigáň, J. Donovalová, V. Szöcs, J. Gašpar, K. Jakusová and A. Gáplovský, *J. Phys. Chem. A*, 2013, **117**, 4870–4883.
26 T. Kobayashi, *J-aggregates*, World Scientific, 1996.
27 R. Fu, B. Xu and D. Li, *Int. J. Therm. Sci.*, 2006, **45**, 841–847.
28 U. Seger-Sauli, M. Panayiotou, S. Schnydrig, M. Jordan and P. Renaud, *Electrophoresis*, 2005, **26**, 2239–2246.
29 J. Crimaldi, *Exp. Fluids*, 2008, **44**, 851–863.
30 S. Ebert, K. Travis, B. Lincoln and J. Guck, *Opt. Express*, 2007, **15**, 15493–15499.
31 V. Natrajan and K. Christensen, *Meas. Sci. Technol.*, 2009, **20**, 015401.